TÜBİTAK

Turkish Journal of Medical Sciences

http://journals.tubitak.gov.tr/medical/

Research Article

Turk J Med Sci
(2015) 45: 372-386
© TÜBİTAK
doi:10.3906/sag-1402-5

Quantitative study of epigenetic signature in head and neck squamous cell carcinoma

Ayesha UMAIR[1,*], Bassel TARAKJI[1], Alzoghaibi IBRAHIM[2], Azzeghaibi NASSER[2], Alenzi FQ[3], Ayesha SHREEN[3]

[1]Department of Oral Maxillofacial Sciences, Al-Farabi College of Dentistry and Nursing, Riyadh, Saudi Arabia
[2]Al-Farabi College of Dentistry, Saudi Arabia, Riyadh, Saudi Arabia
[3]College of Applied Medical Sciences, Salman bin Abdulaziz University, Al-Kharj, Saudia Arabia

Received: 02.02.2014 • **Accepted:** 05.06.2014 • **Published Online:** 01.04.2015 • **Printed:** 30.04.2015

Background/aim: The aberrant upregulation of Forkhead box protein M1 (FOXM1) plays a fundamental role in cancer initiation by perturbing stem cell differentiation. This study aims to investigate the role of FOXM1 in epigenetic modification and gene expression of target genes in primary human oral keratinocytes, squamous cell carcinoma cell lines, and head and neck squamous cell carcinoma (HNSCC) tissue biopsies.

Materials and methods: A genome-wide promoter methylation microarray was used to compare HNSCC cell line (n = 8), primary human oral keratinocytes (NOK; n = 8) transduced with FOXM1 and EGFP, and HNSCC tissue biopsies (n = 3). Seventeen Foxm1B-induced differentially methylated genes were shortlisted. An absolute quantitative polymerase chain reaction was used to validate the differential promoter DNA methylation of each candidate gene induced by FOXM1. These results were compared with the methylation status and altered gene expressions of candidate genes in a panel of genomic DNA and messenger RNA (mRNA) samples previously extracted from HNSCC tissue biopsies.

Results: The results were consistent with our hypothesis, showing that aberrant upregulation of FOXM1 expression in in vitro primary NOK induces a global hypomethylation pattern similar to the HNSCC cell line and has an inverse correlation with in vivo mRNA expression levels of HNSCC tissue biopsy.

Conclusion: Such epigenetic changes have tremendous clinical potential as biomarkers for early cancer detection and therapeutic interventions.

Key words: Forkhead box protein M1, epigenetic modifications, gene expression

1. Introduction

1.1. Head and neck squamous cell carcinoma

Cancers in the head and neck region are mostly referred to as head and neck squamous cell carcinoma (HNSCC). HNSCC is the fifth most common cancer and the sixth most common cause of mortality in the world. In 2007, according to the National Cancer Institute Surveillance Epidemiology and End Result cancer statistic review, 34,360 individuals were predicted to be diagnosed with HNSCC (http://seer.cancer.gov/). This has raised severe health concerns in the public all over the world.

There are various risk factors that are associated with HNSCC. These factors encompass environmental factors as well as personal lifestyles. Heavy alcohol consumption, smoking tobacco, and chewing of betel quid with tobacco are the established risk factors (1). Other predisposing factors include dietary factors such as consumption of processed meats and red meat; lack of iron and essential vitamins A, C, and E; exposure to UV light; and viral strains, e.g., human papilloma virus (HPV), herpes simplex, and the Epstein–Barr virus. These risk factors cause cancer by bringing about epigenetic changes and genetic mutations. Forkhead box protein M1 (FOXM1) is upregulated in a majority of human cancers (2,3). It has been established that FOXM1 is upregulated early in human squamous cell carcinoma (4). Recently, FOXM1's role in the initiation of cancer by perturbing stem cell differentiation was identified (5). Abnormal epigenetic modification such as DNA methylation and demethylation is implicated in the pathogenesis of solid tumors. These epigenetic changes occur early during cancer stem cell initiation (6). The link between epigenetic abnormalities and cancer evolution is becoming clearer day by day. Research in the field of head and neck cancers has shown significant advancement

* Correspondence: ayesha_khan23@live.com

in the last few decades. Detection of HNSCC at an early stage can increase survival by up to 80%, hence suggesting that the early detection of stable markers such as DNA methylation markers can provide immense assistance in the diagnosis, treatment, and prediction of recurrence of HNSCC.

1.2. Epigenetics

Epigenetics refers to heritable and stable changes in gene expression without alteration in primary DNA sequences. These changes are brought about by different epigenetic mechanisms such as DNA methylation or methylation, phosphorylation, or acetylation of histone proteins around which the DNA wound itself to form chromatin. Epigenetic regulation controls the cellular RNA expression patterns. Epigenetics is involved in multiple processes such as gene silencing, X chromosome inactivation, paramutation, imprinting, the progress of carcinogenesis, and embryonic development (7,8). Any dysregulation in epigenetic mechanisms may lead to various human diseases, including autoimmune diseases, cancer, and neurological disorders (9). During cancer there is uncontrolled cell growth as cells escape the normal physiological regulation of proliferation, differentiation, and apoptosis. This takes place as a result of the silencing of tumor suppressor genes or abnormal activation of oncogenes. It has been established recently that there are factors other than genetic abnormalities, such as DNA sequence mutation and genomic instability, that lead to cancer predisposition. Here epigenetics comes into play. Research in this new field of science has shown that the early epigenetic alterations are a prerequisite to oncogenic genetic mutations that lead to cancer.

Of the various epigenetic mechanisms, DNA methylation has been intensely investigated. It involves the addition of a methyl group to the 5 position of the cytosine pyrimidine ring. During cell proliferation the DNA methylation pattern is maintained by DNA methyltransferase enzymes (DNMT1, DNMT3a, and DNMT3b) (10,11). DNA methylation plays a major role in normal cellular differentiation and development. Stable change in the methylation status of DNA can alter the gene expression so that the cells have the ability to retain their cellular pattern. Aberrant DNA methylation is associated with malignancies and can occur in 2 forms: global DNA hypomethylation and promoter DNA hypermethylation (12–14). DNA hypomethylation is associated with earlier stages of cancer. It can result in the reactivation of various cancer- and growth-related genes as well as chromosomal instability and genetic mutations, whereas hypermethylation in cancer cells occurs in the promoter regions of CpG islands (15,16) and results in the silencing of tumor suppressor genes. The loss of function of tumor suppressor genes leads to aberrant cell proliferation, lack of DNA repair, apoptosis evasion, and the continuation of the cell cycle even with the presence of damaged DNA, and all of these events lead to genomic instability that occurs due to loss of heterozygosity and chromosomal number abnormality. In normal cells the tumor suppressor genes are unmethylated and hence they are normally transcribed and can perform their functions. Promoter DNA methylation induces the loss of expression of tumor suppressor genes, predisposing transformation of normal cells into oncogenesis.

The other epigenetic mechanism is posttranslational modification of amino acids in histone proteins. Histones are proteins around which DNA wraps itself for compaction. Histone modification appears to work by maintaining and establishing the gene activity states as it controls DNA accessibility. DNA is highly accessible when histone H3 is methylated (H3K4me) and histone H4 is hyperacetylated (H4K16Ac), whereas DNA is inaccessible when histone 3 is methylated on lysine residue 27. The H2A family of histone proteins plays a major role in chromatin reprogramming; damage to this family changes its functions and results in genomic instability and cellular proliferation.

Any dysregulation in the abovementioned chief epigenetic mechanisms can lead to numerous diseases like cancer, autoimmune diseases, and neurological disorders (9). Epigenetic changes are reversible and precede genetic expression; therefore, they are thought to be an earlier mechanism, with an edge over genetics. Epigenetic changes have tremendous potential for the discovery of early cancer biomarkers, essential in screening, diagnosis, prevention, and treatment. For example, cancer can be prevented or treated by reversing cancer-specific epigenetic changes before irreversible mutations take place. Figure 1 illustrates a common alteration in cancer cells: hypermethylation of a tumor's suppressor genes suppresses its transcription, leading to loss of its normal cellular functions.

1.3. Forkhead box M1 transcriptional factor

FOXM1 (previously called HFH-11B, TRIDENT, WIN, MPP2, and FOXM1b) is a protein that is encoded by the *FOXM1* gene in humans. This protein is a member of the FOX family of transcription factors, which includes a minimum of 50 unique *FOX* genes. FOXM1 is present in 3 isoforms: FOXM1A/isoform1, FOXM1B/isoform3, and FOXM1C/isoform2. All 3 isoforms can bind to DNA, but only FOXM1B and FOXM1C act as transactivators and hence can activate their target genes by binding to 5'-A(C/T)AAA(C/T)AA-3' (3). The cellular localization and regulation of FOXM1 is determined by posttranslational modification such as phosphorylation of FOXM1.

FOXM1 protein is highly expressed in actively dividing cells (17), whereas its levels are hardly detectable in terminally differentiated cells (18). This protein plays a key role in cell proliferation, cell growth, development,

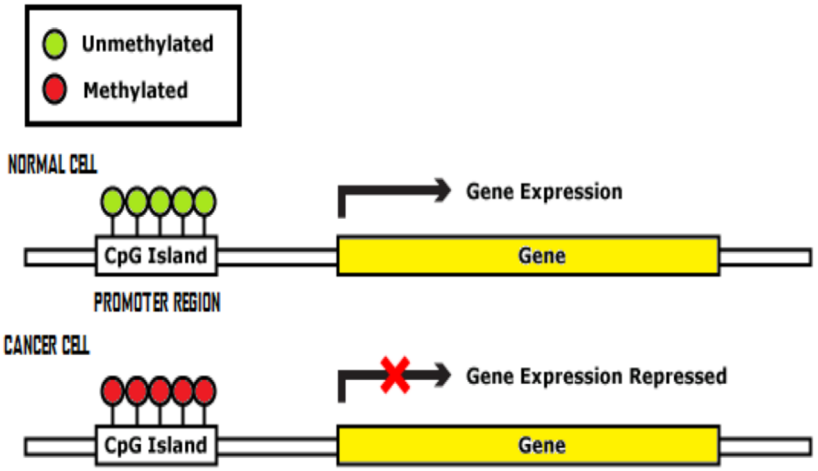

Figure 1. DNA methylation in gene promoter region leads to repression of gene expression.

differentiation, and longevity. Cells lacking the FOXM1 protein show multiple defects, such as chromosomal missegregation, polyploidy, an abnormal number of chromosomes, defects in cytokinesis, and DNA fragmentation. Hence, this suggests a fundamental role for FOXM1 in DNA repair (19) as well as maintaining genomic stability (2).

During embryogenesis FOXM1 expression is induced in a number of tissues, as it plays a vital role in the development of lungs, heart, blood vessels, and the liver. In adult tissues its levels are greatly decreased, but during organ injury and numerous cancers its expression level is high (20). During the cell cycle FOXM1 levels are found to be highest in the S phase and the G2/M phase (3,17). FOXM1 can regulate the expression of multiple cell cycle genes that control the G1/S transition phase, S phase and M phase progression, and G2/M phase and chromosomal segregation. FOXM1 itself is regulated by cell cycle-promoting factors such as cyclin B and cyclin D as well as antiproliferation signals that inhibit cell death, differentiation, and cell cycle arrest (3). Other than cell cycle transition, FOXM1 also plays important roles in DNA damage repair (19), apoptosis (21), tissue regeneration (22), angiogenesis (23), and metastasis (24).

1.4. FOXM1 role in human tumorigenesis

In addition to its key functions in the cell cycle and damaged DNA repair, FOXM1 plays a pivotal role in oncogenesis. FOXM1 is known as a human protooncogene. The first evidence of a link between FOXM1 and cancer was established in 2002, when it was found that in basal cell carcinoma there is abnormal upregulation of FOXM1 (25). Subsequent studies and microarray analyses have shown that FOXM1 is overexpressed in a number of human cancers. Furthermore, it has been established that during head and neck cancer FOXM1 expression is upregulated during the early stages (4). Epithelial stem cells having features like self-renewal, high migration capacity, drug resistance, and high clonogenic potential are susceptible to oncogenic selection and are thought to have a role in the development and maintenance of the majority of tumors. Studies have shown that FOXM1 plays a major role in the regulation of adult epithelial stem cell renewal and differentiation. Recent evidence supports the notion that aberrant upregulation of FOXM1 expression in undifferentiated human keratinocyte stem cells possessing high clonogenic potential leads to a disturbance of epithelial differentiation, leading to formation of hyperproliferative "precancer" stem cells (5). This finding indicates that abnormal upregulation of FOXM1 in normal stem cells leads towards a multistep oncogenic evolutionary pathway.

The role of FOXM1 is not only limited to the initiation of cancer; it also plays an important role in all stages of tumorigenesis, from early predisposition and tumor initiation (5) to cancer progression (4,26) and metastasis (3). There are a number of carcinogenic and environmental factors that activate FOXM1, resulting in uncontrolled cell proliferation and malignant transformation: for example, nicotine in tobacco (4), oxidative stress (27,28), UV light (29), and ionizing irradiation (19). These factors are reported to aberrantly increase FOXM1 expression levels, which induces genomic instability and epigenetic modification by activating downstream targets HELLS and CEP55 protein. HELLS is a helicase required in DNA strand separation, repair, replication, transcription, and epigenetic modification such as DNA methylation. CEP55 is a mitotic phosphoprotein required in cytokinesis (30). It has also been found that the gene locus of FOXM1 (12p13.3) is amplified in HNSCC. All these findings

suggest that aberrant upregulation of FOXM1 expression results in oncogenic genomic instability and enhanced cellular proliferation leading to the development of cancer.

1.5. FOXM1, epigenetics, and HNSCC

Exposure to the various risk factors (e.g., UV light, tobacco, and ionizing radiations) associated with cancer may result in aberrant overexpression of oncogene *FOXM1*. It is also known that the loss of p53 function, c-MYC, RAS, and p16/Rb pathway inactivation in cancer cells lead to constitutive upregulation of FOXM1 (5). FOXM1 is known as a driver mutation, which acts during the early stages of oncogenesis by tumor initiation and predisposition (5). Epigenetic changes occur early in the development of cancer, followed by genetic mutations. FOXM1 initiates cancer by uncontrolled expansion of stem cells and by suppressing their differentiation (5). Aberrant expression of FOXM1 leads to genomic instability and epigenetic reprogramming by activating downstream targets CEP55 and DNMT1. CEP55 causes mitotic instability (4,31), and deregulation of HELLS may lead to altered genomic methylation due to downregulation of DNMT1 and chromatin remodeling (4). This all suggests that abnormal upregulation of FOXM1 brings epigenetic modifications in conjunction with genomic instability, which causes development of a heterogeneous population of abnormal cells that are more likely to acquire properties that lead to the development of cancer.

2. Materials and methods

2.1. Patient nucleic acid samples

The use of human tissue in this study was approved by Barts and the London NHS Trust; the School of Medicine and Dentistry, Queen Mary University of London; and the UK National Research Ethics Committee. All clinical samples, which were additional to diagnosis, were collected according to local ethics committee-approved protocols and written informed patient consent was obtained from all participants.

2.2. Cell culture and viral transduction

The primary normal human oral keratinocytes (OK355, HOKG, OK113, NOK, NOK1, NOK3, NOK16, and NOK376) used in this study were donated by healthy, disease-free individuals undergoing wisdom tooth extraction and were cultured as previously described (4,29). Oral SCC cell line SCC15 (32) is a well-established cell line cultured as described earlier (4,5,29).

In this experiment human primary oral keratinocytes were grown and subsequently transduced by the gene of interest. We used the *FOXM1B* human protooncogene and EGFP (an inert enhanced green fluorescent protein) as controls. In order to make infectious viral particles, retroviral packaging cells (Phoenix A) were first transduced with a retroviral DNA plasmid carrying the gene of interest. Those cells that were unable to be infected by virus were incapable of surviving the antibiotic selection, while the remaining transduced cells were cultured for viral production. A viral supernatant was obtained and was used to transfect the target primary human oral keratinocytes with FOXM1B and EGFP. Retroviral supernatant and transduction procedures were performed using our established protocols (4,5,29). Equal levels of EGFP and FOXM1B expression were achieved by serial retroviral supernatant titration experiment and subsequently EGFP plasmid copy numbers were confirmed by quantitative polymerase chain reaction (qPCR) using genomic DNA extracted from transduced cells according to our previously established method (29). The levels of ectopic FOXM1 expression in the primary keratinocytes were titrated to replicate levels found in cancer cells as reported previously (4,5,29). Transduced cells were cultured for 3–5 days to allow transgene expression prior to experiment.

2.3. Statistical analysis

Statistical analysis was performed with Microsoft Excel using the Student t-test (2-tailed). $P < 0.05$ was considered to be statistically significant.

2.4. Ethical approval

The human tissues used in this study were approved by Barts and the London NHS Trust; School of Medicine and Dentistry, Queen Mary University of London; and the UK National Research Ethics Committee.

2.5. Isolation of methylated genomic DNA

2.5.1. Fragmentation of gDNA

The samples used were DNA from normal oral keratinocytes treated with EGFP, cells infected by FOXM1B, and the HNSCC cell line (SCC15). This genomic DNA was fragmented by treating it with an enzyme according to the manufacturer's protocol. The kit used was the Methyl Collector Ultra (catalogue no. 55005) provided by Active Motif Europe, Belgium.

2.5.2. Enriching methylated gDNA

The following protocol was used to enrich gDNA: a complete binding buffer was prepared, and a high-salt and a low-salt binding buffer were both produced by using reagents supplied in the kit (Table 1).

Next, 10 µL of magnetic beads was added to the required number of PCR tubes for the reaction and components shown in Table 2 were added to the tubes to complete the binding reaction.

The mixture was shaken and incubated for 1 h at 4 °C on a rotisserie shaker. The tubes were then placed on a magnetic stand so that the beads moved to one side and the supernatant that contained the unbound fraction was removed. To resuspend the beads, they were washed with 200 µL of binding buffer and the supernatant was

Table 1. Buffer conditions.

High-salt binding conditions		Low-salt binding conditions	
Reagent	One reaction	Reagent	One reaction
Binding buffer AM7	100 µL	Binding buffer AM12	100 µL
Protease Inhibitor cocktail	0.5 µL	Protease Inhibitor cocktail	0.5 µL
Total volume	100.5 µL	Total volume	100.5 µL

Table 2. Reagents used.

Reagents	One reaction
Magnetic beads	10 µL
Complete binding buffer (high or low salt)	70 µL
Fragmented genomic DNA	From 1 ng to 1 µg (in a final volume of 10 µL)
His-MBD2/MBD3L1 protein complex	10 µL
Total volume	100 µL

removed. To recover the methylated DNA fragments from the beads they were resuspended in 100 µL of complete elusion buffer.

Elusion buffer for each reaction consisted of 2 µL of proteinase K and 98 µL of elusion buffer AM1. Next, it was incubated for 30 min at 50 °C, inverted every 10 min so that the beads were resuspended. Samples were returned to room temperature before the addition of 2 µL of proteinase K stop solution. The stop solution was warmed for 10 min at 37 °C prior to addition. Samples were mixed and then placed on a magnetic stand, the beads moved to one side and the supernatant removed and transferred to new tubes. The supernatant consisted of the methylated gDNA fragments.

2.5.3. DNA clean up

The DNA was cleaned in order to get rid of all protein contaminations necessary before PCR amplification. The protocol used was the phenol/chloroform extraction and ethanol precipitation.

2.6. Microarray and gene selection

A nonbiased genome-wide microarray promoter methylation profiling analysis was performed in order to obtain a list of differentially methylated genes present in the methylation-enriched gDNA and total gDNA that had been extracted and purified from normal primary oral keratinocytes transduced with either EGFP or FOXM1B and the HNSCC cell line (SCC15) as a positive control. The genes that were most significantly differentially methylated by FOXM1B were then identified and short-listed. The list of candidate genes was further validated by using qPCR. This microarray analysis was performed using NimbleGen 720k array chips, which cover 22,532 promoter CpG islands proximal to transcriptional start sites. The service was provided by Roche NimbleGen, Inc., USA. Figure 2 illustrates the selection criteria of candidate genes for this project. The most significantly differentially methylated genes in control cells (NOKG) were identified. These were then compared with gene lists of NOKF and SSC15 cell lines. Genes that showed opposing methylation status between NOKG and NOKF were selected and compared with SCC15 to find the list of common genes between NOKF and SCC15.

2.7. List of target genes and primer sequence

The 17 target genes and primers are given in Tables 3, 4, and 5.

2.8. Real time quantitative PCR (RT-qPCR)

A LightCycler LC480 qPCR machine (Roche Diagnostics Ltd., UK) was used for absolute gene quantification. The SYBR Green (Roche Diagnostics) method was used. It was confirmed that the PCR primers used only produced a single peak. The 2 most stable reference housekeeping genes used were *YAP1* and *POLR2A*.

2.9. qPCR workflow

Melting peak analysis was performed to verify the specificity of PCR primers. Ten-fold serial dilutions of the amplified products were prepared in t-RNA solution (Sigma). Absolute quantification for a single target gene was achieved by creating standard curves. These were then stored in the LC480 analysis software program for future sample analysis. Each PCR experiment consisted of

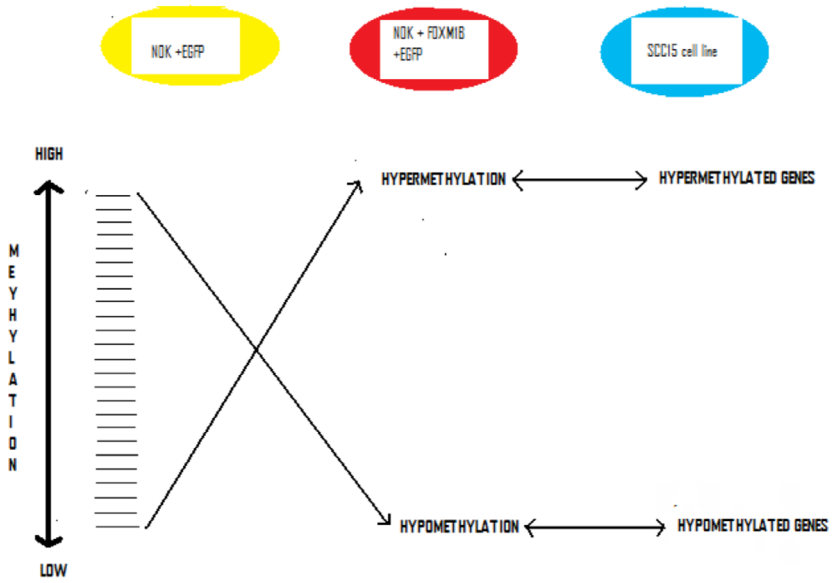

Figure 2. Selection of FOXM1B induced differentially methylated genes. The most significantly differentially methylated genes in control cells (yellow) were identified. These were then compared with a gene list of FOXM1B (blue) and SSC15 (orange) cell lines. Genes that showed opposing methylation status between control cell line and FOXM1B transduction cell line were selected and compared with SCC15 to find the list of common genes between FOXM1B-treated cell lines and SCC15.

Table 3. Hypermethylated genes.

Size (bp)	Gene	Primer sequence
110	*gTET3-F*	aggtgcacagagtgcgagt
	gTET3-R	gcctattgctctgctcttgc
76	*gTAS2R60 -F*	ccatggatgctcttcagctc
	gTAS2R60-R	acattctgtggttgcctatgaa
95	*gFSTL3-F*	aaaagtgcccctaggttggt
	gFSTL3-R	cttgagtctttatttccttggtgag
93	*gPDGFB-F*	tcccacctactgcactttcc
	gPDGFB-R	aaaggaaagcccccaaaaat
102	*gGNG13-F*	ggccccactcacaacatct
	gGNG13-R	aggcgtggtctcacaggata
94	*gNXPH2 -F*	tgagaccccatacttatcttctgg
	gNXPH2-R	gggcttgtttctttgtcattcta
89	*gATF6B-F*	tggtgagctgctgcatattt
	gATF6B-R	acttcccttgtcccacctg
123	*gFKBPL-F*	tgctagggcagcctcagt
	gFKBPL-R	ctttttccaggttcccaagg

Table 4. Hypomethylated genes.

Size (bp)	Gene	Primer sequence
86	*gGLT8DI-F*	gcgacgctctagcggtta
	gGLT8DI-R	cgagcacacttgccctct
80	*gSPCS1-F*	cgcgcaagtactgtcaagg
	gSPCS1-R	gaagtgttcgccgtcagtg
80	*gFABP6-F*	tgacctatgagcgcgtgagc
	gFABP6-R	ttttattggtgggtttgtagctc
93	*gOR3A1-F*	agctgcagtcctgcgaat
	gOR3A1-R	ccatagaatatggcaaccacag
93	*gDNAJC17-F*	gatgcagcaggaagaccag
	gDNAJC17-R	aaatttattggtgacgttgaagaa
92	*gTBC1D10B-F*	gctcagctggggtctctgt
	gTBC1D10B-R	caccccctgggatgacaac
112	*gB4GALT2-F*	ggggcttggatcagtaagtct
	gB4GALT2-R	ctaaagcacccacacaaagat
76	*gRAB4OB-F*	agggaagaaaatgccaaagat
	gRAB4OB-R	agctcttccttgacctgtcg
81	*gBMP1-F*	attcctcaccaagctcaacg
	gBMP1-R	tgccagatgcagttcttgtt

Table 5. Housekeeping genes.

POLRA2-F	GCAAATTCACCAAGAAGAGACG
POLRA2-R	CACGTCGACAGGAACATCAG
YAP1-F	CCCAGATGAACGTCACAGC
YAP1-R	GATTCTCTGGTTCATGGCTGA

a standard concentration of 10^5 copies of target genes and housekeeping genes in order to find out the copy number of target genes in each unknown gDNA or cDNA sample. The LC480 software automatically calculates the gene copy number present in unknown samples by comparing it with the calibrated standard (10^5 copies) respective to that of previously stored standard curve for each target gene. A Microsoft Excel spreadsheet was used for data calculation and analysis.

3. Results

3.1. Gene expression quantification using qPCR

To quantify the exact mRNA copy number of target genes in the FOXM1B-transduced cells and cancer cell lines, we produced standard curves by using known DNA concentrations (copy number). Amplification curves and melting analyses were performed for all the target genes. Melting analysis determines PCR product specificity by showing only one peak, whereas amplification curves help to produce standard curves to determine PCR efficiency and curve fitting errors to allow accurate calculation of target gene concentrations in unknown samples, based on the Roche Light Cycler480 operating software internal algorithm. *YAP1* and *POLR2A* were used as housekeeping genes, as they have been previously shown to be stably expressed in both normal and cancer cells (4).

3.2. Target genes table

In this study 17 target genes were investigated. Table 6 is a compilation of all the target genes. These details were taken from the standard curve produced for each candidate gene.

3.3. Correlation between promoter methylation and gene expression

It is known that differential promoter hypermethylation leads to silencing of gene expression whereas hypomethylation causes upregulation of gene expression. In this project we used an absolute qPCR to first validate

Table 6. Target gene standard curve metadata.

	Gene	Size (bp)	Tm	Primer dimer	Error	Efficiency
1.	*TET3*	110	92.31	-	0.00859	1.796
2.	*TAS2R60*	76	82.69	-	0.00106	1.850
3.	*FSTL3*	95	90.27	-	0.0290	1.564
4.	*PDGFB*	93	82.53	-	0.0083	2.131
5.	*GNG13*	102	88.48	-	0.0401	1.774
6.	*NXPH2*	94	81.20	-	0.00860	1.797
7.	*ATF6B*	89	82.47	-	0.00823	1.912
8.	*FKBPL*	123	90.21	-	0.00512	1.906
9.	*GLT8D1*	86	91.10	-	0.0279	1.939
10.	*SPCS1*	80	88.59	-	0.0214	2.050
11.	*FABP6*	80	88.50	-	0.00818	1.938
12.	*OR3A1*	93	85.85	-	0.00886	1.714
13.	*DNAJ17*	93	87.00	-	0.0950	1.652
14.	*TBC1D10B*	92	87.00	-	0.00835	1.992
15.	*BMP1*	81	91.20	-	0.0413	2.230
16.	*B4GALT2*	112	85.60	-	0.0277	1.952
17.	*RAB40B*	76	81.60	-	0.0137	1.889

the differential methylation of genes in methylated gDNA collected from our control primary normal human oral keratinocytes, expressing either EGFP (NOKG) or FOXM1 (NOKF) SCC15 cell lines, and in methylated gDNA and cDNA collected from tissue biopsy of 3 pairs of normal margin and oral SCC cells. The absolute qPCR measured and compared the relative methylation and gene expression of the 17 candidate FOXM1B-induced differentially methylated genes that were identified from the microarray study. These genes showed the parallel deferential gene expression in both cultured cells and in patient tumor tissues. According to our hypothesis, if the shortlisted 17 target genes were involved in oncogenesis, then their promoter methylation status would modify the gene expression in the cancer tissues as well. In order to support our hypothesis we performed absolute qPCR to measure the gene expression of these candidate genes in 3 pairs of normal margin and HNSCC biopsy tissues. Once their gene expression levels were obtained we next correlated them with the promoter DNA methylation status of these genes in FOXM1B-transduced cells.

3.4. DNA methylation vs. mRNA expression in NOKF

To validate if the candidate genes were indeed differentially methylated in FOXM1-transduced cells (NOKF), methylation (using gDNA) and gene expression (cDNA) were quantified for each gene in NOKG and NOKF. Differential methylation and gene expression were then calculated for each gene as a ratio of NOKF:NOKG and plotted as a correlation chart between gene expression and relative methylation. Figure 3 shows that there is an inverse correlation between promoter methylations and their respective gene expressions in FOXM1B-transduced cells, with a regression coefficient R^2 value of 0.564. Each data point with an error bar represents the mean ± SEM of 3 NOKF samples. A positive control gene, *CDKN2A/p16*, known to be hypermethylated by FOXM1B, was included in this study. This negative correlation is in agreement with our hypothesis. According to this graph, the methylation status of target genes from the microarray analysis is consistent with the qPCR results.

3.5. DNA methylation vs mRNA expression in SCC cell lines

Using the same validation strategy as above, the candidate genes were subsequently validated in SCC15 cell lines. Similarly, Figure 4 shows a negative relation between the promoter DNA methylation and relative mRNA expression in the SCC15 cell line with a regression coefficient R^2 of 0.502.

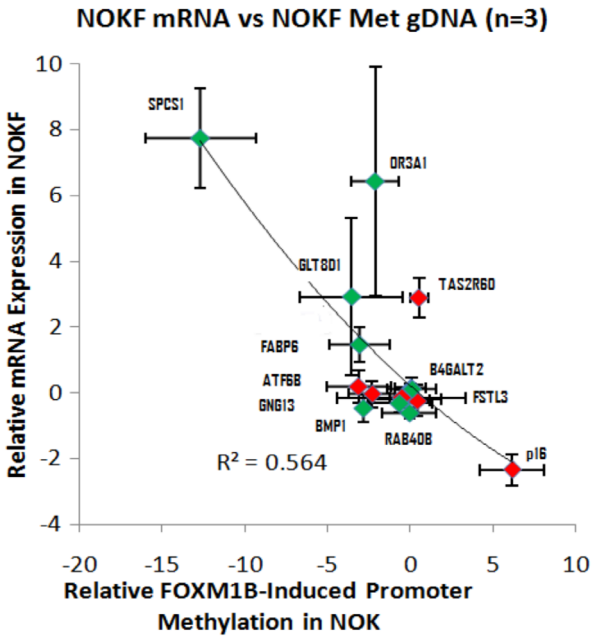

Figure 3. Inverse correlation between FOXM1B-induced promoter methylation in NOK and relative mRNA expression in NOKF. Green dots represent hypomethylated genes and red dots hypermethylated genes.

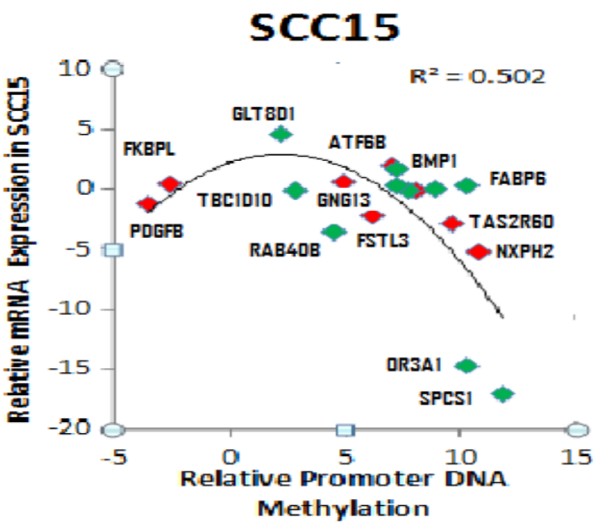

Figure 4. Promoter DNA methylation vs. relative mRNA expression in SCC15.

3.6. DNA methylation in NOKF vs. relative mRNA expression in HNSCC cell lines

We next investigated whether the candidate gene expression pattern was a common phenomenon across different HNSCC cell lines. There were 8 samples used (SCC15, 5PT, VB6, SqCC/Y1, SVpgC2a, SVFN4, SVFN5, and SVFN10). cDNAs were prepared from these 8 independent HNSCC cell lines and then compared with DNA methylation status for each candidate gene. Figure 5 shows the inverse correlation between the promoter methylation status in FOXM1B-induced cells, NOKF, and the corresponding gene expression in HNSCC cell lines. The regression coefficient R^2 was 0.849. This graph indicates that the candidate genes selected from FOXM1B-induced cells behaved the same in HNSCC cell lines.

3.7. Correlation between NOKF and tissue biopsies

Having established that the candidate differentially methylated genes showed inverse gene expression patterns in HNSCC cell lines, we next investigated if this trend persisted in in vivo HNSCC tumor biopsy tissues as well. First, the relative methylation status of each gene was compared between gDNA extracted from NOKF and HNSCC tissues. Three pairs of tissue biopsy samples were used. In Figure 6A there is a positive correlation between promoter methylation of NOKF and HNSCC tissue biopsies' gDNA, with a correlation coefficient of R^2 = 0.637. This indicates that the methylation signature found

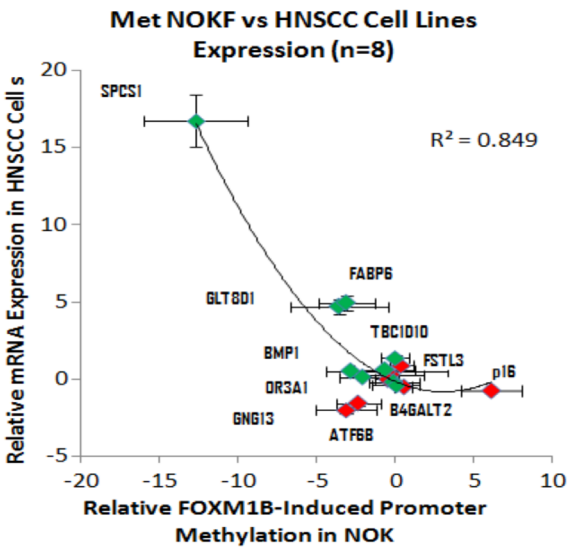

Figure 5. Correlation between FOXM1B-induced promoter methylation in NOK and relative mRNA expression in HNSCC cell lines (n = 8).

in NOKF appears to be similar to that found in HNSCC tumor tissues.

To further validate that the differential methylation signature indeed resulted in inverse gene expression in the tumor tissues, the gene expressions of each of the candidate genes were quantified and compared between the 3 pairs

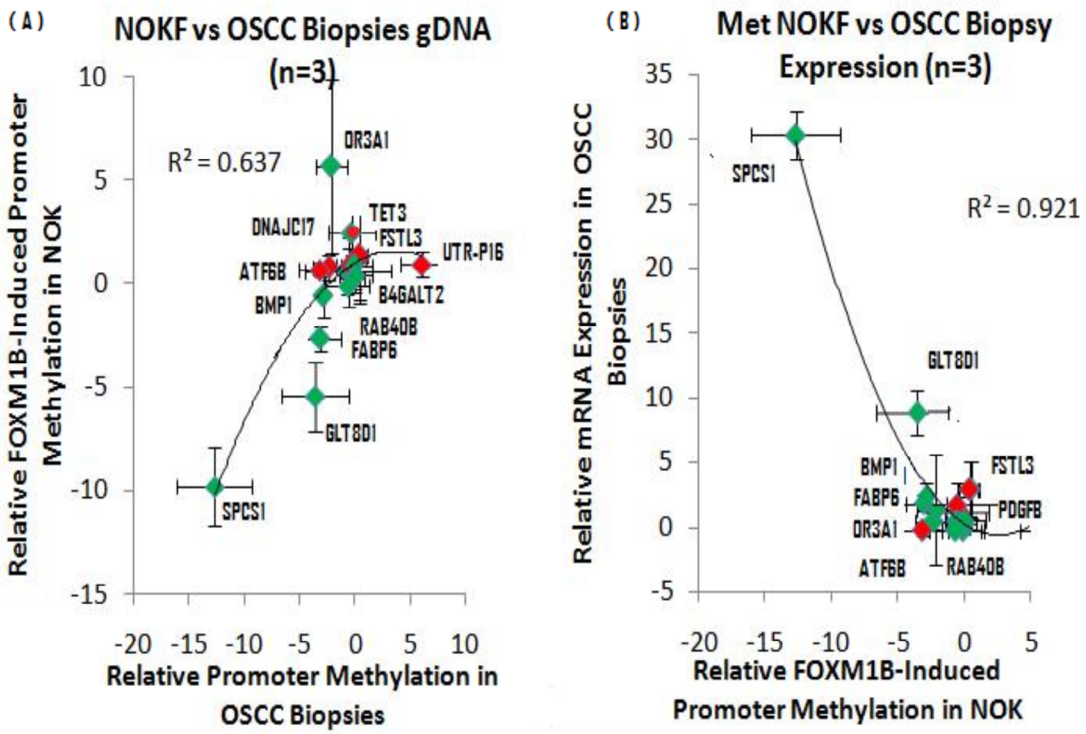

Figure 6. A) Correlation between the relative promoter methylation in NOKF and HNSCC biopsy tumor tissues. **B)** Promoter DNA methylation in NOKF cells and its corresponding mRNA expression in HNSCC biopsies.

of normal margin and HNSCC tumor tissues. In Figure 6B an inverse correlation is shown between promoter methylation in NOKF and its corresponding mRNA expression in HNSCC tissues. The correlation coefficient R^2 is 0.921. This graph provides data that seem to be in agreement with our hypothesis that FOXM1 induces a cancer-like methylation signature. As stated previously, if the candidate genes were involved in oncogenesis, we hypothesized that their promoter methylation status would change the mRNA expression in tumor tissues.

3.8. Correlation between DNA methylation and relative mRNA expression in individual patient samples

Although the candidate genes showed differential gene expression in the HNSCC tumor samples, the methylation statuses of these genes in the tumor samples were not known. In order to investigate this, gDNA from the same 3 pairs of normal margin and tumor tissues were analyzed for differential methylation. Figures 7A–7C show 3 patient samples, A, B, and C. These graphs illustrate the inverse correlation of individual patient between promoter DNA methylation and relative mRNA expression.

Figure 7D shows the average association between the methylation status and the corresponding cDNA expression in all 3 patient samples. In the graph of patient A, all genes other than OR3A1 behaved as expected, hence giving an inverse relation value for R^2 of 0.972. The genes that were hypomethylated were highly expressed, such as, for example *SPCS1* and *GALT8D1*, whereas the hypermethylated genes showed low levels of expression of their respective genes, for example *PDGFB* and *TET3*.

The graph for patient B also shows a negative relation, with a regression coefficient R^2 value of 0.577. *FKBPL* showed an opposing DNA methylation status, which related well to its mRNA expression. Other hypermethylated genes, such as *TAS2R60*, *PDGFB*, *FSTL3*, and *UTR-p16*, showed downregulation of respective gene expression, whereas the hypomethylated genes such as *SPCS1*, *OR3A1*, *GLT8D1*, and *FABP6* showed corresponding gene upregulation.

For patient C, an inverse relation was seen with regression coefficient R^2 of 0.760. In this graph the methylation statuses of a few genes were not consistent with the microarray results, as these genes showed opposing methylation statuses, for example *FSTL3*, *PDGFB*, *TAS2R60*, and *OR3A1*. Nevertheless, genes *FSTL3*, *PDGFB*, and *TAS2R60* showed DNA hypomethylation, but these 3 genes correlated well to their respective gene expression, whereas *OR3A1* showed DNA hypermethylation and corresponding gene expression downregulation.

In Figure 7D, all 3 patients' data were averaged to obtain the combined result of the relationship between the promoter DNA methylation and respective mRNA expression levels. As expected, a negative correlation between methylation and gene expression was obtained, having a regression coefficient of 0.954.

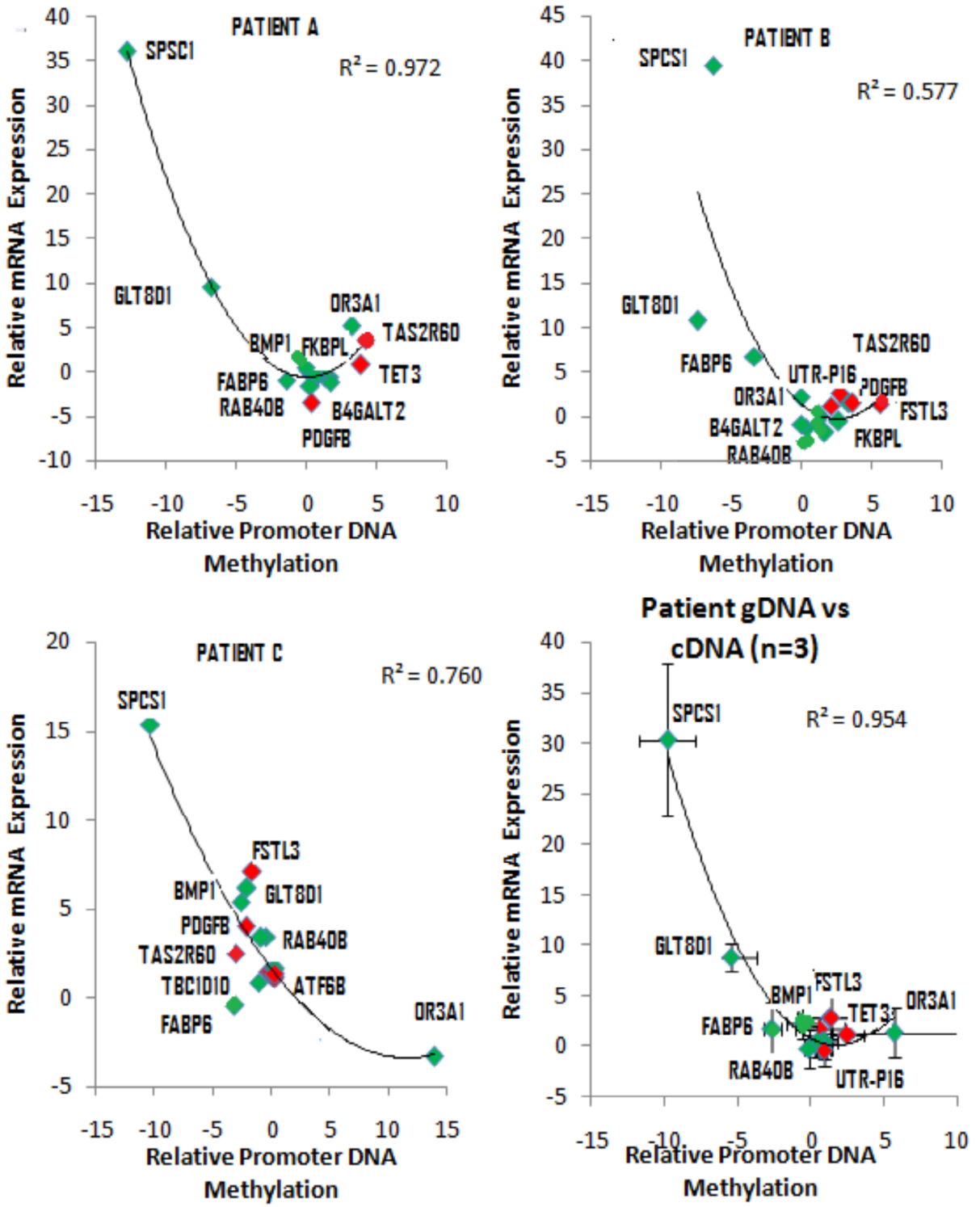

Figure 7. Correlation between DNA methylation and relative mRNA expression in individual patient samples **(A–C)** and averaged data for 3 patients **(D)**.

4. Discussion

FOXM1, an important transcription factor for the regulation of cell cycle, cell division, genomic stability, aging, and development, has been found to be ubiquitously upregulated in many human cancers. It is known that FOXM1 expression is upregulated early

during HNSCC carcinogenesis (4). The understanding of the early mechanism of cancer initiation can help us find effective interventions for cancer prevention and cure. FOXM1's role in cancer initiation by perturbing stem cell renewal has been recently established (5). Epigenetic modifications like DNA methylation and demethylation are also known to occur early during cancer (6). It is hence important to know whether FOXM1 has a role in epigenetic modification that initiates cancer formation. We hypothesize that upregulation of FOXM1 induces cancer-inducing epigenetic modifications such as DNA methylation and demethylation. In order to support our hypothesis we analyzed a list of differentially methylated genes that had been shortlisted after performing a genome-wide microarray promoter DNA methylation study. The promoter DNA methylation pattern and corresponding mRNA expression of each candidate gene is measured in normal primary oral keratinocytes with increased FOXM1expression by using real-time absolute qPCR and is then compared to HNSCC cell lines, HNSCC biopsy cDNA samples, and a normal control.

An absolute qPCR was used to obtain a standard curve for each candidate gene so that accurate levels of promoter DNA methylation and the respective mRNA expression could be measured. First, to validate that the target genes were indeed differentially methylated in FOXM1-transduced cells, the promoter methylation and relative gene expression were quantified for each gene in control cells (NOKG) and NOKF. The data obtained showed that the microarray analysis was mostly consistent with the qPCR results, whereby the methylation status of each gene was inversely correlated with gene expression. An inverse relation was obtained with a correlation coefficient of R^2 = 0.564 (about 56%). Two genes, *ATF6B* and *GNG13*, that were expected to be hypermethylated did not exhibit the strong status that was seen in microarray gene expression for *FOXM1* and *SCC15*, but nevertheless their respective mRNA expressions were consistent with their DNA methylation status. This highlights the importance of validating microarray results using qPCR. A positive control gene, *p16*, which is known to be a tumor-suppressor gene, was included in this study. It was shown from the results that this gene was hypermethylated in NOKF and in the majority of HNSCC cell lines and tumor tissues and, correspondingly, its mRNA expression levels were suppressed. The *p16* gene has a regulatory role in the cell cycle. It stabilizes the tumor suppressor gene *p53*, which controls apoptosis (32). Mutation of this gene increases the risk of developing cancer. It can cause downregulation of genes and impairment of the retinoblastoma pathway (33), of which CDK4 has a role, and p16 has a regulatory function over CDK4. Silencing of the gene *p16* has been associated with numerous cancer cell lines. It is found to be inactive in HNSCC and is associated with advanced stages of this type of cancer (34). The silencing of *p16* as a result of induced hypermethylation by FOXM1 may promote cancer development and progression.

Next, the candidate genes were subsequently validated in the SCC15 cell line using the same validation strategy as above. An inverse negative correlation between the promoter DNA methylation and relative mRNA expression in the SCC15 cell line, with a regression coefficient R^2 of 0.502 (about 50%) was obtained. Four genes, *PDGFB*, *FKBPL*, *OR3A1*, and *SPCS1*, showed opposing methylation status. However, the mRNA expression of these 4 genes correlates well with their respective promoter methylation status. For example, *SPCS1* and *OR3A1* showed hypermethylation with corresponding downregulation of gene expression. Similarly, *PDGFB* and *FKBPL* showed hypomethylation and upregulation of the relevant gene expression. The *FKBPL* gene encodes a protein that plays a role in immunoregulation and basic cellular processes involving protein trafficking and folding. It is thought to have a role in induced radio resistance and also appears to have involvement in cell cycle (Gene ID 63943, NCBI 2011). The other *PDGFB* gene encodes for a protein that is a member of the platelet-derived growth factor family. Mutations in this gene are associated with meningioma. Reciprocal translocations between chromosomes 22 and 7, at sites where this gene and that for COLIAI are located, are associated with a particular type of skin tumor called dermatofibrosarcoma (Gene ID 5155, NCBI 2011).

To confirm whether the candidate gene expression pattern was a common phenomenon across different HNSCC cell lines, gene expression was measured in 8 independent HNSCC cell lines for correlation with DNA methylation status for each candidate gene. The results indicated that the candidate genes selected from FOXM1B-induced cells showed a similar inverse correlation between methylation and gene expression. A coefficient of R^2 = 0.845 (about 85%) was obtained. This was true except for 2 genes, *GNG13* and *ATF6B*, which showed promoter hypomethylation in NOKF and low levels of their corresponding gene expression in HNSCC cell lines. Their methylation status did not match their respective mRNA expression levels. The candidate differentially methylated genes showed inverse gene expression pattern in HNSCC cell lines. In order to investigate if the same trend persisted in HNSCC tumor biopsy tissues we compared the relative methylation status of each gene between gDNA extracted

from NOKF and HNSCC tissue. A positive correlation with a coefficient of $R^2 = 0.637$ (about 64%) was obtained. *OR3A1* showed promoter hypermethylation status in NOKF with a corresponding low expression of mRNA, whereas hypomethylation in HNSCC was consistent with gene expression. The data indicated that the methylation signature found in NOKF appear to be similar to that found in HNSCC tumor tissues. Next, the gene expressions of each of the candidate genes were quantified and compared between the 3 pairs of normal margin and HNSCC tumor tissues to validate that the differential methylation signature indeed resulted in inverse gene expression in the tumor tissues. There was an inverse correlation between promoter methylation in NOKF and its corresponding mRNA expression in HNSCC tissues, with a correlation coefficient of $R^2 = 0.921$ (about 92%). This shows that FOXM1 induces a cancer-like methylation signature.

To investigate the level of heterogeneity within each patient, an individual patient's methylation status and gene expression was studied for each candidate gene. In patient A, an inverse relation of R^2 value of 0.972 was obtained. The *OR3A1* gene showed hypermethylation, which was the same as in NOKF, but it did not correspond with its respective gene expression. In patient B, a regression coefficient R^2 value of 0.577 was obtained. *FKBPL* showed opposing DNA methylation status, but it related well to its mRNA expression. In patient C, the methylation statuses of a few genes were not consistent with the microarray results. *FSTL3*, *PDGFB*, *TAS2R60*, and *OR3A1* genes showed opposing methylation status but correlated well with their respective gene expression. These results demonstrated an interpatient heterogeneity with certain candidate genes. Nevertheless, the overall trends of methylation and gene expression were consistent with our hypothesis that FOXM1 induced a cancer-like methylation pattern that is found in tumor biopsy tissues. In the end, we averaged the data of the 3 patients to obtain a combined result of the relationship between the promoter DNA methylation and respective mRNA expression levels. As expected, a negative correlation between methylation and gene expression was obtained, having a regression coefficient of 0.954 (about 95%).

Modifications in genomic methylation status may be an enhancing factor in the oncogenesis process, and evidence shows that global DNA hypomethylation might contribute to genomic instability and increased mutation rate (35). Wide-spread global hypomethylation is accompanied with hypermethylation in a few genes and an increase in DNMT1, an enzyme responsible for regulating promoter methylation (36).

DNA methylation has emerged as a highly promising biomarker and is being actively studied in multiple cancers, and a large number of potential biomarkers have been identified. In prostate cancer the hypermethylation of the glutathione-S-transferase pi gene has emerged as a good diagnostic marker (37). This project can help us find good biomarkers for the early detection of HNSCC. In this study most of the candidate genes showed differential methylation status in both FOXM1-transduced cells and in HNSCC when compared to normal control cells. These genes may have a clinical potential for early diagnosis of cancer as well as prognosis and therapeutic treatments. By detecting the methylation status of various genes we can measure the level of genomic instability in cells, which may guide us into cancer prognostics. It is well known that tumor suppressor genes are hypermethylated and hence silenced in cancer, and the use of demethylating drugs, which could interact with enzymes such as DNA methyltransferase, can play a fundamental role in the therapeutic treatment of cancer. Procaine is one such drug that has been found to have growth inhibitory effects on human cancer cells. In the future we may be able to prevent cancer by arresting the reversible epigenetic modifications before irreversible mutation takes place.

In summary, this study shows that upregulation of FOXM1 leads to cancer-like epigenetic alterations in normal primary human oral keratinocytes. The differentially methylated genes selected from microarray analysis were validated using qPCR. Genes with promoter hypermethylation showed corresponding low levels of mRNA expression and hypomethylated genes showed elevated levels of relative gene expression. The same pattern was observed in HNSCC cell lines as well as in HNSCC tumor biopsy samples. We need further studies to confirm the mechanism of epigenetic modifications and the role of each gene in cancer initiation. Future proposed experiments include the following aims:

1. To investigate the mechanism by which FOXM1 causes differential promoter methylation of candidate genes.

2. To investigate the role of the differentially methylated genes in cancer initiation and progression.

3. To investigate whether the genes identified in this study could be used in clinical practice as early detection biomarkers and for cancer prognostics. Further clinical samples validation studies would be required to establish their clinical use.

Acknowledgment

This study was done as a part of a thesis submitted to the Queen Mary University of London, UK.

References

1. Daly B, Watt RG, Batchelor P, Treasure ET. Oral Cancer Prevention in Essential Dental Public Health. 1st ed. Oxford, UK: Oxford University Press; 2003.
2. Laoukili J, Stahl M, Medema RH. FoxM1: at the crossroads of ageing and cancer. Biochim Biophys Acta 2007; 1775: 92–102.
3. Wierstra I, Alves J. FOXM1, a typical proliferation-associated transcription factor. Biol Chem 2007; 388: 1257–1274.
4. Gemenetzidis E, Bose A, Riaz AM, Chaplin T, Young BD, Ali M, Sugden D, Thurlow JK, Cheong SC, Teo SH et al. FOXM1 upregulation is an early event in human squamous cell carcinoma and it is enhanced by nicotine during malignant transformation. PLoS One 2009; 4: e4849.
5. Gemenetzidis E, Elena-Costea D, Parkinson EK, Waseem A, Wan H, Teh MT. Induction of human epithelial stem/progenitor expansion by FOXM1. Cancer Res 2010; 70: 9515–9526.
6. Yamada Y, Watanabe A. Epigenetic codes in stem cells and cancer stem cells. Adv Genet 2010; 70: 177–199.
7. Bird A. DNA methylation patterns and epigenetic memory. Genes Dev 2002; 16: 6–21.
8. Meissner A, Mikkelsen TS, Gu H, Wernig M, Hanna J, Sivachenko A, Zhang X, Bernstein BE, Nusbaum C, Jaffe DB et al. Genome-scale DNA methylation maps of pluripotent and differentiated cells. Nature 2008; 454: 766–770.
9. Portela A, Esteller M. Epigenetic modifications and human disease. Nat Biotechnol 2010; 28: 1057–1068.
10. Okano M, Bell DW, Haber DA, Li E. DNA methyltransferases Dnmt3a and Dnmt3b are essential for de novo methylation and mammalian development. Cell. 1999; 99: 247–257.
11. Okano M, Xie S, Li E. Cloning and characterization of a family of novel mammalian DNA (cytosine-5) methyltransferases. Nat Genet 1998; 19: 219–220.
12. Herman JG, Baylin SB. Gene silencing in cancer in association with promoter hypermethylation. N Engl J Med 2003 Nov; 349: 2042–2054.
13. Feinberg AP, Tycko B. The history of cancer epigenetics. Nat Rev Cancer 2004; 4: 143–153.
14. Esteller M. Epigenetics in cancer. N Engl J Med 2008; 358: 1148–1159.
15. Zardo G, Tiirikainen MI, Hong C, Misra A, Feuerstein BG, Volik S, Collins CC, Lamborn KR, Bollen A, Pinkel D et al. Integrated genomic and epigenomic analyses pinpoint biallelic gene inactivation in tumors. Nat Genet 2002; 32: 453–458.
16. Esteller M, Corn PG, Baylin SB, Herman JG. A gene hypermethylation profile of human cancer. Cancer Res 2001; 61: 3225–3229.
17. Leung TW, Lin SS, Tsang AC, Tong CS, Ching JC, Leung WY, Gimlich R, Wong GG, Yao KM. Over-expression of FoxM1 stimulates cyclin B1 expression. FEBS Lett 2001; 507: 59–66.
18. Korver W, Schilham MW, Moerer P, van den Hoff MJ, Dam K, Lamers WH, Medema RH, Clevers H. Uncoupling of S phase and mitosis in cardiomyocytes and hepatocytes lacking the winged helix transcription factor Trident. Curr Biol 1998; 8: 1327–1330.
19. Tan Y, Raychaudhuri P, Costa RH. Chk2 mediates stabilization of the FoxM1 transcription factor to stimulate expression of DNA repair genes. Mol Cell Biol 2007; 27: 1007–1016.
20. Kalin TV, Ustiyan V, Kalinichenko VV. Multiple faces of FoxM1 transcription factor: lessons from transgenic mouse models. Cell Cycle 2011; 10: 396–405.
21. Madureira PA, Matos P, Soeiro I, Dixon LK, Simas JP, Lam EW. Murine gamma-herpesvirus 68 latency protein M2 binds to Vav signaling proteins and inhibits B-cell receptor-induced cell cycle arrest and apoptosis in WEHI-231 B cells. J Biol Chem 2005; 280: 37310–37318.
22. Kalinichenko VV, Lim L, Shin B, Costa RH. Differential expression of forkhead box transcription factors following butylated hydroxytoluene lung injury. Am J Physiol Lung Cell Mol Physiol 2001; 280: 695–704.
23. Wang Z, Banerjee S, Kong D, Li Y, Sarkar FH. Down-regulation of Forkhead Box M1 transcription factor leads to the inhibition of invasion and angiogenesis of pancreatic cancer cells. Cancer Res 2007; 17: 8293–8300.
24. Dai B, Kang SH, Gong W, Liu M, Aldape KD, Sawaya R, Huang S. Aberrant FoxM1B expression increases matrix metalloproteinase-2 transcription and enhances the invasion of glioma cells. Oncogene 2007; 26: 6212–6219.
25. Teh MT, Wong ST, Neill GW, Ghali LR, Philpott MP, Quinn AG. FOXM1 is a downstream target of Gli1 in basal cell carcinomas. Cancer Res 2002; 62: 4773–4780.
26. Waseem A, Ali M, Odell EW, Fortune F, Teh MT. Downstream targets of FOXM1: CEP55 and HELLS are cancer progression markers of head and neck squamous cell carcinoma. Oral Oncol 2010; 7: 536–542.
27. Li SK, Smith DK, Leung WY, Cheung AM, Lam EW, Dimri GP, Yao KM. FoxM1c counteracts oxidative stress-induced senescence and stimulates Bmi-1 expression. J Biol Chem 2008; 283: 16545–16553.
28. Park HJ, Carr JR, Wang Z, Nogueira V, Hay N, Tyner AL, Lau LF, Costa RH, Raychaudhuri P. FoxM1, a critical regulator of oxidative stress during oncogenesis. EMBO J. 2009; 28: 2908–2918.
29. Teh MT, Gemenetzidis E, Chaplin T, Young BD, Philpott MP. Upregulation of FOXM1 induces genomic instability in human epidermal keratinocytes. Mol Cancer 2010; 9: 45.
30. Van der Horst A, Simmons J, Khanna KK. Cep55 stabilization is required for normal execution of cytokinesis. Cell Cycle 2009; 8: 3742–3749.

31. Laoukili J, Kooistra MR, Brás A, Kauw J, Kerkhoven RM, Morrison A, Clevers H, Medema RH. FoxM1 is required for execution of the mitotic programme and chromosome stability. Nat Cell Biol 2005; 7: 126–136.

32. Rheinwald JG, Beckett MA. Tumorigenic keratinocyte lines requiring anchorage and fibroblast support cultured from human squamous cell carcinomas. Cancer Res 1981; 41: 1657–1663.

33. Macdonald F. Molecular Biology of Cancer. Oxford, UK: Oxford University Press; 2005.

34. Martinez JC, Palomino JC, Samaniego R, Sepulveda JM, Cabello A, Ricoy JR. Retinoblastoma (Rb) tumor-suppressor pathway alterations in meningeal hemangiopericytomas: High E2F transcription factor 1 expression and loss of Rb expression: study by double immunofluorescence staining and laser-scanning confocal microscopy. Cancer 2008; 113: 166–174.

35. Yuen PW, Man M, Lam KY, Kwong YL. Clinicopathological significance of p16 gene expression in the surgical treatment of head and neck squamous cell carcinomas. J Clin Pathol 2002; 55: 58–60.

36. Chen RZ, Pettersson U, Beard C, Jackson-Grusby L, Jaenisch R. DNA hypomethylation leads to elevated mutation rates. Nature 1998; 395: 89–93.

37. Baylin SB, Herman JG, Graff JR, Vertino PM, Issa JP. Alterations in DNA methylation: a fundamental aspect of neoplasia. Adv Cancer Res 1998; 72: 141–196.

38. Nakayama M, Gonzalgo ML, Yegnasubramanian S, Lin X, De Marzo AM, Nelson WG. GSTP1 CpG island hypermethylation as a molecular biomarker for prostate cancer. J Cell Biochem 2004; 91: 540–552.